


Article

Performance Comparison of Different Modulation Formats for a 40 Gbps Hybrid Optical CDMA/DWDM System against ISI and FWM

Naif Alsowaidi ^{1,*}, Tawfig Eltaif ^{2,*}  and Mohd Ridzuan Mokhtar ³

¹ School of Engineering, University of Tasmania, Hobart, TAS 7001, Australia

² Faculty of Engineering Technology and Science, Higher Colleges of Technology, Madinat Zayed Campus, Abu Dhabi P.O. Box 25026, United Arab Emirates

³ Faculty of Engineering, Multimedia University, Cyberjaya 63100, Malaysia

* Correspondence: naif.alsowaidi@utas.edu.au (N.A.); tefosat@ieee.org (T.E.)

Abstract: This paper carries out a numerical simulation investigating three different modulation formats: carrier suppressed return to zero (CSRZ), modified duobinary return to zero (MDRZ) and return to zero (RZ). The purpose of this investigation is to find the optimum modulation format for the hybrid optical code division multiple accesses–dense wavelength division multiplexing (optical CDMA/DWDM) system with the implementation of an electro-optic phase modulator (EOPM) at a data rate of 40 Gbps per channel, with a transmitted power of 22 dBm and transmission distance of 105.075 km. The results revealed that CSRZ was superior to MDRZ and RZ and was more tolerant to optical fiber nonlinearity. Furthermore, unlike the DWDM systems, the performance of the proposed hybrid system based RZ format was better than the performance of MDRZ. Hence, the CSRZ modulation format is the best candidate for the optical CDMA/DWDM with EOPM module due to its high performance.

Keywords: optical CDMA; DWDM; RZ; MDRZ; CSRZ; FWM; ISI; EOPM



Citation: Alsowaidi, N.; Eltaif, T.; Mokhtar, M.R. Performance Comparison of Different Modulation Formats for a 40 Gbps Hybrid Optical CDMA/DWDM System against ISI and FWM. *Photonics* **2022**, *9*, 555. <https://doi.org/10.3390/photonics9080555>

Received: 30 June 2022

Accepted: 2 August 2022

Published: 7 August 2022

Publisher's Note: MDPI stays neutral with regard to jurisdictional claims in published maps and institutional affiliations.



Copyright: © 2022 by the authors. Licensee MDPI, Basel, Switzerland. This article is an open access article distributed under the terms and conditions of the Creative Commons Attribution (CC BY) license (<https://creativecommons.org/licenses/by/4.0/>).

1. Introduction

A recent Cisco's forecast report stated that the number of devices connected to the internet will be more than three times the worldwide population by 2023 [1]. Therefore, the increase in demand for unlimited bandwidth has led to the evolution of high-capacity and high-speed optical transmission systems to satisfy the ever-growing capacity requirements. A variety of multiplexing techniques have been used to provide the required high-speed transmission. For instance, speed is an advantage obtained from using the time division multiplexing (TDM) system. However, TDM uses one wavelength for downstream and another wavelength for upstream, limiting the optimum bandwidth for a given user. Therefore, the bandwidth of the single fiber is not fully utilized. To compensate for this, the wavelength division multiplexing (WDM) system, which is considered the most successful technique in optical networks [2,3], assigns a specific wavelength for a given subscriber. Despite this advantage in increasing capacity, WDM lacks wavelength sharing and suffers from nonlinear effects. On the other hand, optical code division multiple accesses (optical CDMA) have several key features, most notably, their highly flexible and efficient asynchronous access for multiple users in a busy network, fast scheduling without buffering time, and easier expansion in network implementation. However, optical CDMA suffer from various types of noise, one of which is multiple access interference (MAI), the main source of bit error. To deal with the limitations and inefficiency that arises from each system mentioned above, hybrid systems have been proposed. The hybrid system of optical CDMA–dense wavelength division multiplexing (optical CDMA/DWDM) combines the advantages and strengths of both multiplexing schemes [2,4–7] but still suffers from

limitations such as chromatic dispersion (CD), laser phase noise (LPN) and nonlinear effects as do all the previous systems. These limitations have a huge impact on the signal quality and degrade system performance.

A variety of methods have been proposed to compensate for chromatic dispersion, such as using digital filters including the time-domain least mean square adaptive filter, a time-domain fiber dispersion finite impulse response filter, and a frequency-domain blind look-up filter [7] and by controlling the grating length of the fiber Bragg grating (FBG) [8,9].

The phase noise, which occurs due to transmit and receive lasers, has a huge impact on coherent systems employing high order modulation formats. The appearance of transmit and receive phase noises make it very difficult to discriminate between them. Giulio et al. proposed a digital coherence enhancement (DCE) technique using an interferometric device along with a very simple electronic processing, which significantly reduced the phase noise of transmit or receive lasers [10].

However, when the interactions between the chromatic dispersion and the laser phase noise occurred, they produced a new issue that was very difficult to compensate for. The interaction is called equalization enhanced phase noise (EENP) [11]. A deep investigation on the impact of EENP on nonlinear optical fibers through split-step Fourier simulations has been conducted and analytical model predictions have been proposed for single and multiple channels of a dual-polarization DP-16QAM system over the long haul. The investigation proved that the reducing the EENP had a huge impact on improving the system performance [12].

In addition, nonlinear effects such as inter- and intra-channel Four Wave Mixing (FWM) are considered a major source of impairments in high data rate and high-capacity optical networks [12,13]. In fact, inter- and intra-channel FWM effects have been widely investigated in pure WDM systems and are considered one of the foremost application issues in optical fiber networks [14–18]. On the other hand, the effects of inter- and intra-channel FWM in the hybrid optical CDMA/DWDM system have not been addressed.

Recently, a hybrid optical CDMA/DWDM system considering the effects of inter- and intra-channel FWM and inter-symbol interference (ISI) was proposed [19]. The analysis revealed that the generated inter-channel FWM effect contributes not only as an additional crosstalk component, but also produces other noise terms, namely, signal-FWM, Multiple Access Interference (MAI-FWM), and FWM-FWM noise. It has been shown that the CDMA technology, where the bit's energy is spread over the identification code sequence, could minimize the effect of inter-channel FWM. In addition, the electro-optic phase modulator (EOPM) is used to suppress the intra-channel FWM effect in the hybrid optical CDMA/DWDM system [19].

To implement systems that can support a high data rate, the focus should be more on the modulation formats and line coding, which are used to mitigate the linear and nonlinear impairments of fiber optic transmission [20]. DWDM has been analyzed under the influence of the FWM effect using different modulation formats such as carrier suppressed return to zero (CSRZ) [21], modified duobinary return to zero (MDRZ) [22], differential phase shift keying (DPSK) [23,24], and differential quadrature phase shift keying (DQPSK) [25]. All the modulation formats were proposed as alternative formats to return to zero (RZ) and non-return to zero (NRZ) [26–28].

By extending the work in [18], the target of this paper is to examine the impact of different types of modulation formats (namely return to zero (RZ), carrier suppressed RZ (CSRZ) and the modified duobinary RZ (MD-RZ) formats-based OOK signaling) on the bit error rate (BER) as a key figure of merit performance of the hybrid optical CDMA/DWDM system. The influence of inter- and intra-channel FWM, ISI, and MAI have been considered.

2. Signal Generators and System Description

The proposed hybrid optical CDMA/DWDM system's operational diagram is shown in Figure 1, which consists of K number of channels (i.e., channels) spaced by 0.2 nm at a data rate of 40 Gbps per channel, where each is split into M branches, and each branch

represents one user's data. The user's data are modulated to generate an RZ/CSRZ and MD-RZ optical signal, which then moves to optical CDMA encoding using a multi-diagonal (MD) sequence code. Interested readers may refer to [26–28] for more information about the generation of RZ, MDRZ, and CSRZ. The M optical CDMA users' data are combined by an optical combiner. Then the K channels are multiplexed by the WDM multiplexer followed by EOPM to modulate simultaneously the signal's phase at frequency equal to a single channel's data rate. Further details about the function of EOPM are reported in ref. [19]. The output of the EOPM is then launched into single mode fiber + dispersion compensating fiber (SMF + DCF) followed by a preamplifier to compensate the loss. Noting that each channel could support M number of optical CDMA users, the total number of users that the proposed hybrid system can accommodate is $K \times M$ users.

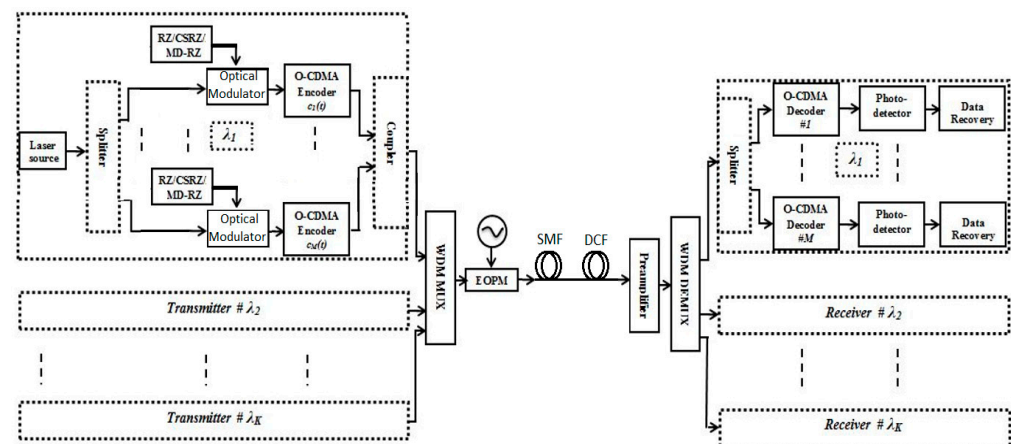


Figure 1. Hybrid Optical CDMA–DWDM system's operational diagram. Single mode fiber (SMF) and dispersion compensating fiber (DCF).

3. Performance Analysis

This section comprises a theoretical analysis of the hybrid optical CDMA/DWDM system performance under the influence of inter- and intra-channel FWM, receiver noise, and MAI. Considering the intensity modulation/direct detection (IM/DD) transmission based on CSRZ signaling, the hybrid system accommodates K channels; each channel carries M optical CDMA users; hence, the data corresponding to the m th user in k th channel are

$$d_k^m(t) = \sqrt{P_t} b_k^m(t) \cos^2 \left[\frac{\pi}{2} (\sin(\pi Bt) + 1) \right] \text{ where, } 0 < t \leq T \quad (1)$$

where $b_k^m(t)$ is the data of the m th user in the k th DWDM channel.

For optical CDMA user's signatures, several address codes can be used, including m sequence, double padded-modified prime code (DPMPC), modified quadratic congruence (MQC), extended grouped new modified prime code (EG-nMPC) and multi-diagonal (MD) code [29,30]. Among all these codes, MD offers the best performance when MAI is considered due to the zero cross-correlation property of MD, where the length of the MD sequences is $F = M \times w$, [31].

Hence, the signature code of the m th user in k th channel is

$$C^{km}(t) = \sum_{f=1}^{M \times w} C_f^{km} P(t - fT_c) \quad (2)$$

where $C^{km} \in \{0, 1\}$ and $P(t)$ refers to the unit rectangular pulse with T_c duration.

All M encoded users' data are combined, where the encoded optical CDMA signals corresponding to k th channel are mathematically expressed as:

$$S_k(t) = \sum_{m=1}^M \sum_{f=1}^{M \times w} \sqrt{P_t} b_k^m(t) C_f^{km} P(t - fT_c) \cos^2 \left[\frac{\pi}{2} (\sin(\pi Bt) + 1) \right] \quad (3)$$

Finally, all the K channels are multiplexed, where each channel consisting of M optical CDMA users is

$$S(t) = \sum_{k=1}^K S_k(t) \quad (4)$$

Then, the output of the DWDM multiplexer is sent over to an EOPM to modulate simultaneously the signal's phase at frequency equal to a single channel's data rate, where such a process helps to suppress the effect of intra-channel FWM. Therefore, the phase of each channel is modulated as:

$$\varphi(t) = \varphi_{\text{EOPM}} \sin(2\pi f_{\text{SCS}} t) \quad (5)$$

where φ_{EOPM} and f_{SCS} are the phase deviation and the frequency of the sinusoidal clock signal, respectively. The output of the EOPM is then transmitted over the SMF as

$$S(t) = \left[\sum_{k=1}^K S_k(t) \right] e^{j\varphi(t)} \quad (6)$$

where, the q th channel signal of the m th user at the DWDM de-multiplexer's output is

$$r_i(t) = \sum_{m=1}^M \sum_f^{M \times w} \sqrt{P_{s,qm}} b_q^m(t) C_f^{qm} \cos(\theta_q) + \sqrt{P_q^{\text{FWM}}} \cos(\theta_q - \theta_{\text{FWM}}) \quad (7)$$

where $P_s = \frac{P_r}{M \times w}$, P_r , b_q^m , and $P_q^{\text{FWM}} = \sum_{abc} P_{\text{OCDMA-DWDM}}^{abc}$ are the received power, the data bit of the m th user in the q th channel, and the total power of generated FWM products at f_q , respectively.

The generated FWM power at frequencies f_a , f_b , and f_c is [32]

$$P_{\text{OCDMA-DWDM}}^{abc} = \frac{\eta}{9} (dy)^2 \left(\frac{P_a}{N} \right) \left(\frac{P_b}{N} \right) \left(\frac{P_c}{N} \right) \exp[-\alpha L] \left[\frac{(1 - e^{-\alpha L})^2}{\alpha^2} \right] \quad (8)$$

where η is the FWM efficiency and can be expressed as [33].

$$\eta = \frac{\alpha^2}{\alpha^2 + (\Delta\beta)^2} \left[1 + \frac{4e^{-\alpha L} \sin^2 \left(\frac{\Delta\beta L}{2} \right)}{(1 - e^{-\alpha L})^2} \right] \quad (9)$$

$\Delta\beta$ is the phase mismatch [32]

$$\Delta\beta = \frac{2\pi\lambda^2}{c} (\Delta f_{ac}) (\Delta f_{bc}) \left[D_C + \left(\frac{\lambda^2}{2c} \right) (SD) (\Delta f_{ac} + \Delta f_{bc}) \right] \quad (10)$$

where d , L , γ , α , P_p , P_q , P_r , α , D_c , and SD are the degeneracy factor; the transmission length; the nonlinearity coefficient; the attenuation of the fiber; the transmitted power per channel; and the chromatic and slope dispersion, respectively.

Considering that the desired user is the first user in the q th DWDM channel, then the received optical field at the photodetector of the first user in the q th DWDM channel after the decoding process is

$$E(t) = E_{q1}(t) + E_{q,\text{MAI}}(t) + E_{q,\text{FWM}}(t) \quad (11)$$

The first, second, third, fourth, and fifth terms in Equation (11) are the electric field of the first user in the q th channel; the electric field of the MAI, and the total electric field of FWM at f_q , respectively.

The total signal current can be derived as

$$i_b(t) = \frac{\Re w P_{r,qb}}{M \times w} + \frac{\Re}{M \times w} \sum_{m=j+1}^M P_{r,qm} b_q^m I_{qm,j}(t_{qm,j}) + i_{\text{FWM}}(t) + i_{sh}(t) + i_{th}(t) \quad (12)$$

The first term in Equation (12) is the desired signal, the MAI component is represented in the second term; while the third, fourth, and fifth terms are due to the FWM, shot, and thermal noises, respectively. Then,

$$\begin{aligned} i_{\text{FWM}}(t) &= 2\Re P_q^{\text{FWM}}(t) \cos^2(\theta_q - \theta_{\text{FWM}}) + 2\Re \sqrt{\frac{P_{r,q1}}{M \times w}}(t) P_q^{\text{FWM}}(t) \cos(\theta_q) \cos(\theta_q - \theta_{\text{FWM}}) \\ &+ 2\Re \sum_{m=j+1}^M \sqrt{\frac{P_{r,qm}}{M \times w}} I_{qm,j}(t_{qm,j}) P_q^{\text{FWM}}(t) \cos(\theta_q) \cos(\theta_q - \theta_{\text{FWM}}) \end{aligned} \quad (13)$$

where the first, second, and third terms represent the mean current of FWM, the signal-FWM, and MAI-FWM, respectively.

The signal current for bit ‘1’ is

$$\begin{aligned} i(1) &= \frac{\Re w P_{r,q1}}{M \times w} + \frac{\Re}{M \times w} \sum_{m=j+1}^M P_{r,qm} I_{qm,j}(t_{qm,j}) + 2\Re P_q^{\text{FWM}}(1) \cos^2(\theta_q - \theta_{\text{FWM}}) \\ &+ 2\Re \sqrt{\frac{P_{r,q1}}{M \times w}} P_q^{\text{FWM}}(1) \cos(\theta_q) \cos(\theta_q - \theta_{\text{FWM}}) \\ &+ 2\Re \sum_{m=j+1}^M \sqrt{\frac{P_{r,qm}}{M \times w}} I_{qm,j}(t_{qm,j}) P_q^{\text{FWM}}(1) \cos(\theta_q) \cos(\theta_q - \theta_{\text{FWM}}) + i_{sh}(1) + i_{th}(t) \end{aligned} \quad (14)$$

The mean and variances for bit ‘1’ are

$$\langle i(1) \rangle = \Re w P_{r,q1} + \Re \langle P_q^{\text{FWM}} \rangle \quad (15)$$

$$\sigma^2(1) = \frac{\Re^2}{(M \times w)^3} \sum_{m=j+1}^M P_{r,qm}^2 + \sigma_{\text{signal-FWM}}^2(1) + \sigma_{\text{MAI-FWM}}^2(1) + \sigma_{sh}^2(1) + \sigma_{th}^2(1) \quad (16)$$

where

$$\sigma_{\text{signal-FWM}}^2(1) = \frac{2\Re^2 P_{r,q1}}{M \times w} \left\{ \frac{1}{8} \sum_{a \neq b \neq c} P_q^{\text{FWM}} + \frac{1}{4} \sum_{a=b \neq c} P_q^{\text{FWM}} + \frac{1}{4} \sum_{a \neq b \neq c=q} P_q^{\text{FWM}} \right\} \quad (17)$$

and

$$\sigma_{\text{MAI-FWM}}^2(1) = \frac{2\Re^2}{(M \times w)^2} \sum_{m=j+1}^M P_{r,qm} \left\{ \frac{1}{8} \sum_{a \neq b \neq c} P_q^{\text{FWM}} + \frac{1}{4} \sum_{a=b \neq c} P_q^{\text{FWM}} + \frac{1}{4} \sum_{a \neq b \neq c=q} P_q^{\text{FWM}} \right\} \quad (18)$$

The mean and variance values for bit “0” are

$$\langle i(0) \rangle = \Re \langle P_q^{\text{FWM}}(0) \rangle \quad (19)$$

$$\sigma^2(0) = \sigma_{\text{MAI-FWM}}^2(0) + \sigma_{\text{FWM-FWM}}^2(0) + \sigma_{sh}^2(0) + \sigma_{th}^2(1) \quad (20)$$

where

$$\sigma_{\text{MAI-FWM}}^2(0) = \frac{2\Re^2}{(M \times w)^2} \sum_{m=j+1}^M P_{r,qm} \left\{ \frac{1}{8} \sum_{a \neq b \neq c} P_q^{\text{FWM}} + \frac{1}{4} \sum_{a=b \neq c} P_q^{\text{FWM}} \right\} \quad (21)$$

Then, the bit error rate (BER), following [34,35] is

$$\text{BER} = Q\left(\frac{\langle i(1) \rangle - \langle i(0) \rangle}{\sigma(1) + \sigma(0)}\right) \quad (22)$$

4. Results and Discussion

In total, 15 DWDM channels with a spacing of 0.2 nm operating at the c-band, where each channel carries eight users, can be accommodated by the proposed hybrid system, a data rate of 40 Gbps and transmission power of 22 dBm transmitted over 105.075 km. The SMF with the following properties: cross effective area of $80 \mu\text{m}^2$ and chromatic and slope dispersion of $16.75 \text{ ps/nm}\cdot\text{km}$ and $0.075 \text{ ps/nm}^2\cdot\text{km}$ was used to evaluate the performance of the hybrid system along with the DCF.

The EOPM module is used to simultaneously modulate the signals' phase, which are carried by the DWDM channels to eradicate the intra-channel FWM effect. The eradication of intra-channel FWM occurs because its contributions coming from different pulses acquire a relative phase shift. By optimizing this phase shift, destructive interference can be obtained between different intra-channel FWM contributions. The key EOPM parameter is the phase deviation, which determines the relative phase shift of the intra-channel FWM contributions. In Ref. [19], the optimum phase deviation of the EOPM module was set at $2\pi/3$.

To guarantee the avoidance of ISI, the authors in [19] proposed the squeezing method, where its principle is to squeeze the identification sequence code interval into less than a bit duration; therefore, in this paper we implemented the squeezing method where the code sequence interval was squeezed into 25% of bit duration to guarantee the avoidance of the ISI.

In this paper, the simulation was conducted using co-simulation of OptSim and MATLAB software utilizing SMF and DCF with the properties stated in Table 1.

Table 1. Hybrid System Properties.

Parameter	Value	Parameter	Value
Number of channels	$N = 15$	Dispersion slope for SMF	$0.075 \text{ ps/nm}^2\cdot\text{km}$
Number of users per channel	$K = 8$	Cross effective area for SMF	$80 \mu\text{m}^2$
Channel spacing	0.2 nm	Length of DCF	15.075 km
Data rate per channel	40 Gbps	Attenuation for DCF	0.5 dB/km
Data rate per user	5 Gbps	Dispersion for DCF	$-100 \text{ ps/nm}\cdot\text{km}$
CW DFB Laser launch power	9.8 dBm	Dispersion slope for DCF	$-0.45 \text{ ps/nm}^2\cdot\text{km}$
Total insertion losses	30.8 dBm	Cross effective area for DCF	$22 \mu\text{m}^2$
Preamplifier gain	30 dB	Nonlinear refractive index	$2.6 \times 10^{-20} \text{ m}^2/\text{W}$
Total transmitted power to the fiber	22 dBm	Max nonlinear phase shift	3.14 mrad
Length of SMF	90 km	Phase deviation of EOPM	$\varphi_{\text{EOPM}} = \frac{2\pi}{3}$
Attenuation for SMF	0.2 dB/km	Length and weight of the sequence code	$F = 24, w = 3$
Dispersion for SMF			$16.75 \text{ ps/nm}\cdot\text{km}$

Based on the mathematical model presented in Section 3, the strength of the FWM depends not only on the fiber characteristics but also on the optical sequence code properties, such as code length, weight, and auto/cross correlation, where longer sequence code lengths are recommended for achieving better performance. Therefore, the identification sequence code not only has a positive/negative impact on MAI but also has an impact on the effect of FWM. Whether it impacts positively or negatively depends on the properties of the optical sequence code. The MD code is one of the best candidates to use as a signature sequence code for the optical CDMA users in our proposed hybrid system. The performance of the proposed hybrid system for CSRZ, MDRZ, and RZ modulation formats in terms of the BER as a function of transmitted power at $w = 3$ and $F = 24$ for the MD sequence code are shown in Figure 2, Figure 3, and Figure 4, respectively.

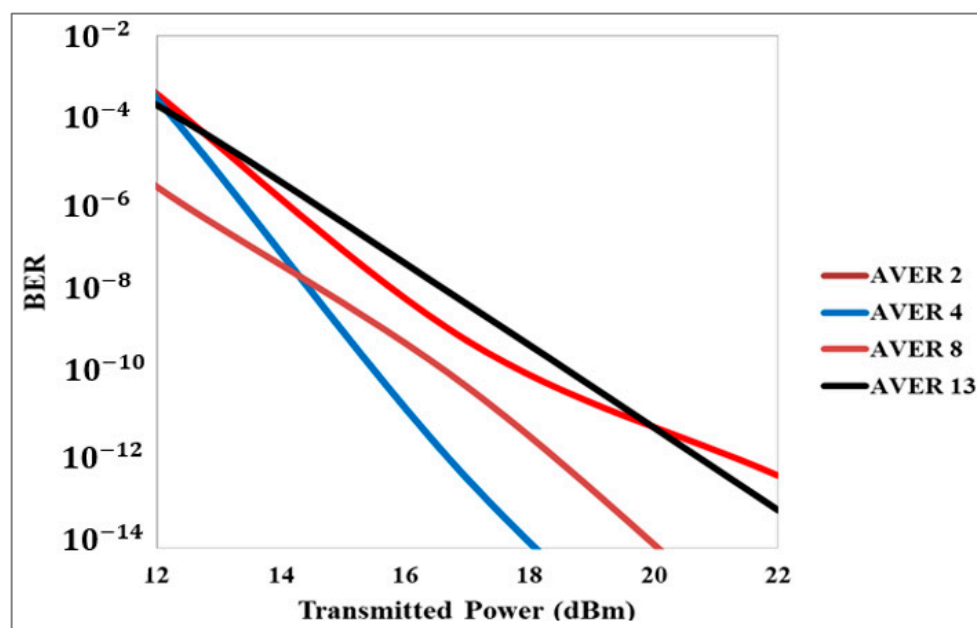


Figure 2. The Average BERs versus Transmitted Power for Four Random Channels (CSRZ).

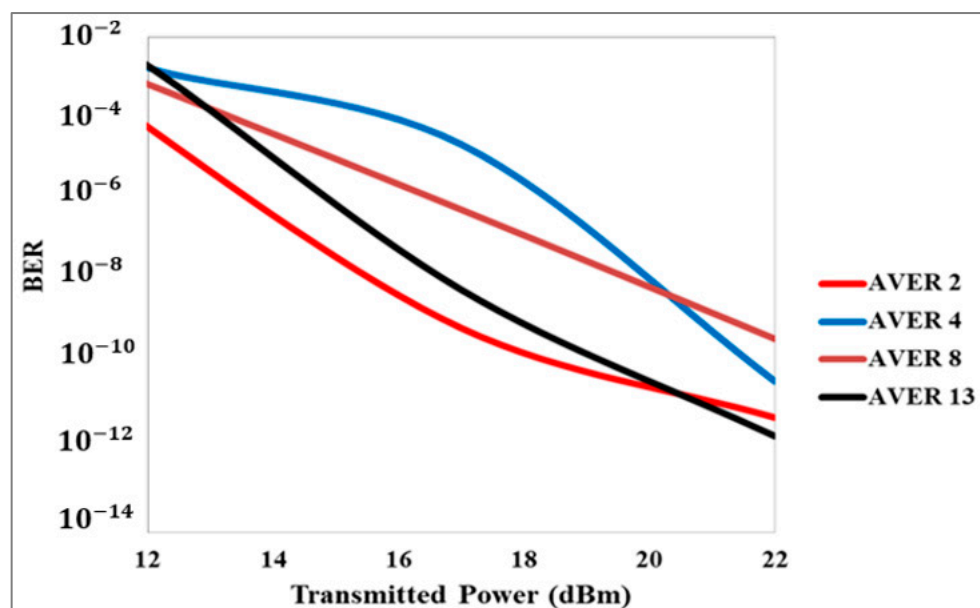


Figure 3. The Average BERs versus Transmitted Power for Four Random Channels (MDRZ).

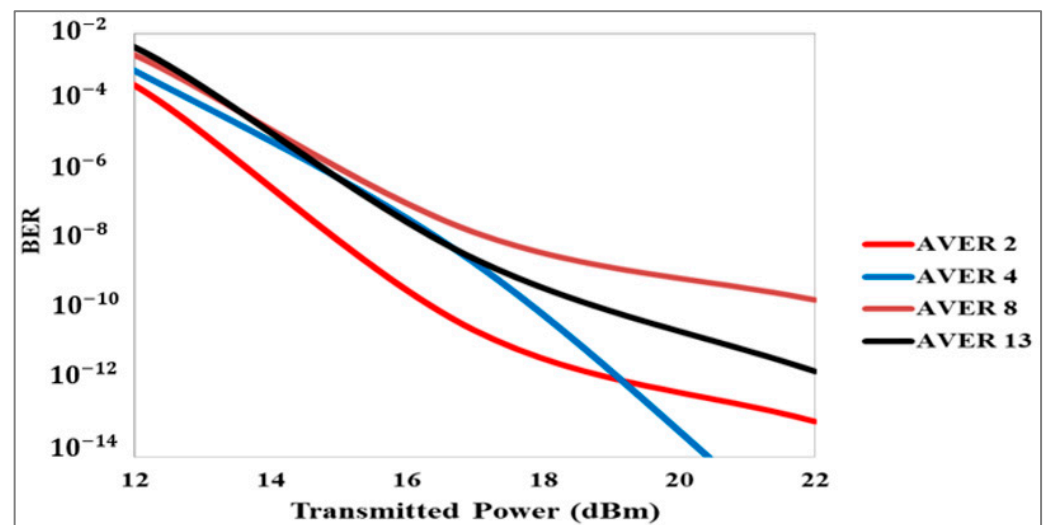


Figure 4. The Average BERs versus Transmitted Power for Four Random Channels (RZ).

The CSRZ achieved a significant improvement over RZ and MDRZ with the implementation of EOPM as shown in Figure 5. This is because the optical phase in a CSRZ signal is periodic at half the data rate and the interaction between the neighboring pulses is suppressed [20]. In other words, its carrier suppression and the π phase change between alternative pulses help to suppress the interference between the pulses [14]. This was previously observed and has been attributed to the fact that CSRZ is more tolerant to optical fiber nonlinearity [20,22,36].

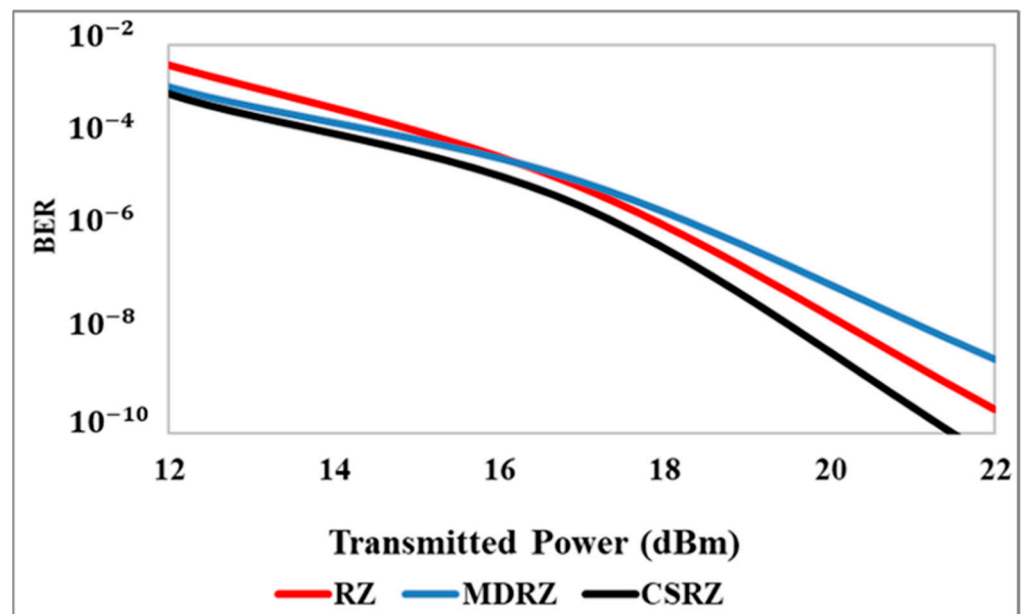


Figure 5. Comparison between Different Modulation Formats' Performances for the Hybrid Optical CDMA/WDM System.

On the other hand, it was reported in the literature that the performance of MDRZ in purely WDM systems outperformed the RZ modulation format [37]; however, in the proposed hybrid system using the EOPM module, the performance of the system based on the RZ format had better performance than the one based on the MDRZ format, as shown in Figures 3 and 4. The average BERs of channels 2, 8, and 13 at a transmitted power of 22 dBm for MDRZ were 5.93×10^{-12} , 4.8×10^{-10} , and 2.1×10^{-12} , and for RZ, they were 9.82×10^{-14} , 2.75×10^{-10} , and 2.6×10^{-12} , respectively. The EOPM module was used

to simultaneously modulate the signals' phase carried by DWDM channels to eradicate the intra-channel FWM effect. The eradication of intra-channel FWM occurs because its contributions coming from different pulses acquire a relative phase shift. In ref. [19] the optimum phase deviation of the EOPM module was set at $2\pi/3$, which helped to destroy the interference between different intra-channel FWM contributions. Thus, the phase shift was responsible for reducing the intra-channel FWM effect, which in turn lowered the bit error.

The effectiveness of the EOPM module was more significant in the case of the CSRZ modulation formats compared to RZ and MDRZ formats. These findings of the current study are consistent with those in ref. [20].

5. Conclusions

In conclusion, following the theoretical analysis on the hybrid optical CDMA/DWDM system, it was found that the EOPM module was more effective using the CSRZ modulation format compared to the MDRZ and RZ modulation formats. This is due to the phase shift introduced by the EOPM between the pulses. The phase shift is responsible for reducing the intra-channel FWM effect, as the destructive interference can be achieved between different pulses by optimizing the phase shift. The simulation results indicated that the strength of the FWM effect depends on the optical signature code properties, where the longer code is better. The phase deviation of the EOPM module is the key parameter that plays a crucial role in eradicating the effect of intra-channel FWM.

Author Contributions: Conceptualization, N.A. and T.E.; methodology, N.A. and T.E.; software, N.A.; validation, N.A. and T.E.; formal analysis, N.A. and T.E.; investigation N.A. and T.E.; writing—original draft preparation, N.A.; writing—review and editing, N.A. and T.E.; visualization, N.A. and T.E.; supervision, T.E. and M.R.M.; project administration, T.E. and M.R.M.; funding acquisition, T.E. and M.R.M. All authors have read and agreed to the published version of the manuscript.

Funding: This work was supported by the Multimedia University (Malaysia), project SAP ID: MMUI/160092.

Institutional Review Board Statement: Not applicable.

Informed Consent Statement: Not applicable.

Data Availability Statement: Not applicable.

Acknowledgments: This work was supported by the Higher Colleges of Technology, United Arab Emirates, for publication sponsorship.

Conflicts of Interest: The authors declare no conflict of interest.

References

1. Cisco Annual Internet Report. Available online: <https://www.cisco.com/c/en/us/solutions/collateral/executive-perspectives/annual-internet-report/white-paper-c11-741490.pdf> (accessed on 14 July 2022).
2. Wang, X.; Wada, N.; Miyazaki, T.; Cincotti, G.; Kitayama, K.-I. Field Trial of 3-WDM \times 10-OCDMA \times 10.71-Gb/s Asynchronous WDM/DPSK-OCDMA Using Hybrid E/D Without FEC and Optical Thresholding. *J. Lightwave Technol.* **2007**, *25*, 207–215. [CrossRef]
3. Kitayama, K.; Wang, X.; Wada, N. OCDMA over WDM PON—A solution path to gigabit-symmetric FTTH-. *J. Lightwave Technol.* **2006**, *24*, 1654. [CrossRef]
4. Chen, H.; Xiao, S.; Zhu, M.; Shi, J.; Bi, M. Hybrid WDMA/OCMD system with the capability of encoding multiple wavelength channels by employing one encoder and one corresponding optical code. *Chin. Opt. Lett.* **2010**, *8*, 745–748. [CrossRef]
5. Huang, J.-F.; Nieh, T.-C.; Chen, K.-S. Structuring waveguide-grating-based wavelength-division multiplexing/optical code division multiple access network codecs over topology of concentric circles. *Opt. Eng.* **2013**, *52*, 015006. [CrossRef]
6. Choi, Y.-K.; Hanawa, M.; Wang, X.; Park, C.-S. Upstream Transmission of WDM/OCMD-PON in a Loop-Back Configuration with Remotely Supplied Short Optical Pulses. *J. Opt. Commun. Netw.* **2013**, *5*, 183–189. [CrossRef]
7. Xu, T.; Jacobsen, G.; Popov, S.; Li, J.; Vanin, E.; Wang, K.; Friberg, A.T.; Zhang, Y. Chromatic dispersion compensation in coherent transmission system using digital filters. *Opt. Express* **2010**, *18*, 16243–16257. [CrossRef] [PubMed]
8. Dar, A.B.; Jha, R.K. Chromatic dispersion compensation techniques and characterization of fiber Bragg grating for dispersion compensation. *Opt. Quantum Electron.* **2017**, *49*, 108. [CrossRef]

9. Pradhan, S.R.; Sahoo, S.R.; Pradhani, G.R.; Panda, T. Chromatic Dispersion Compensation Using Adaptive Fiber Bragg Grating for High-Speed Optical Communication. *ECS Trans.* **2022**, *107*, 7201. [\[CrossRef\]](#)
10. Ghazi, A.; Aljunid, S.A.; Idrus, S.Z.S.; Rashidi, C.B.M.; Al-dawoodi, A.; Mahmood, B.A.; Rafeeq, R.M. A Systematic review of Multi-Mode Fiber based on Dimensional Code in Optical-CDMA. *J. Phys. Conf. Ser.* **2021**, *1860*, 012016. [\[CrossRef\]](#)
11. Colavolpe, G.; Foggi, T.; Forestieri, E.; Secondini, M. Impact of Phase Noise and Compensation Techniques in Coherent Optical Systems. *J. Lightwave Technol.* **2011**, *29*, 2790–2800. [\[CrossRef\]](#)
12. Jin, C.; Shevchenko, N.A.; Li, Z.; Popov, S.; Chen, Y.; Xu, T. Nonlinear Coherent Optical Systems in the Presence of Equalization Enhanced Phase Noise. *J. Lightwave Technol.* **2021**, *39*, 4646–4653. [\[CrossRef\]](#)
13. Xu, T.; Karanov, B.; Shevchenko, N.; Lavery, D.; Liga, G.; Killey, R.I.; Bayvel, P. Digital nonlinearity compensation in high-capacity optical communication systems considering signal spectral broadening effect. *Sci. Rep.* **2017**, *7*, 12986. [\[CrossRef\]](#) [\[PubMed\]](#)
14. Forzati, M.; Berntson, A.; Martensson, J. Asynchronous Phase Modulation for the Suppression of IFWM. *J. Lightwave Technol.* **2007**, *25*, 2969–2975. [\[CrossRef\]](#)
15. Du, J.; Teng, Z.; Shen, N. Semi-analytic modeling of FWM noise in Dispersion-managed DWDM systems with DQPSK/DPSK/OOK channels. *Opt. Commun.* **2016**, *358*, 180–189. [\[CrossRef\]](#)
16. Jiang, L.; Yuan, X.; Cui, Y.; Chen, G.; Zuo, F.; Jiang, C. Optical bistability and four-wave mixing in a hybrid optomechanical system. *Phys. Lett. A* **2017**, *381*, 3289–3294. [\[CrossRef\]](#)
17. Alsowaidi, N.; Eltaif, T.; Mokhtar, M.; Hamida, B.A. Reduction of Four-Wave Mixing in DWDM System Using Electro-Optic Phase Modulator. *Int. J. Electr. Comput. Eng.* **2018**, *8*, 2384–2389. [\[CrossRef\]](#)
18. Lawan, S.; Mohammad, A. Reduction of four wave mixing efficiency in DWDM systems using optimal PMD. *Opt. Quantum Electron.* **2018**, *50*, 91. [\[CrossRef\]](#)
19. Alsowaidi, N.; Eltaif, T.; Mokhtar, M. Suppression of Inter and Intra Channel Four Wave Mixing effect in Optical CDMA over DWDM Hybrid System. *Chin. Opt.* **2019**, *12*, 156–166. [\[CrossRef\]](#)
20. Winzer, P.J.; Essiambre, R.J. Advanced Optical Modulation Formats. *Proc. IEEE* **2006**, *94*, 952–985. [\[CrossRef\]](#)
21. Forzati, M. Phase Modulation Techniques for On-Off Keying Transmission. In Proceedings of the 9th International Conference on Transparent Optical Networks, Rome, Italy, 1–5 July 2007.
22. Sharan, L.; Shanbhag, A.G.; Chaubey, V.K. Design and simulation of modified duobinary modulated 40 Gbps 32 channel DWDM optical link for improved non-linear performance. *Cogent Eng.* **2016**, *3*, 1256562. [\[CrossRef\]](#)
23. Kassa-Baghdouche, L.; Simohamed, L.M. Performance limitations of an optical RZ-DPSK transmission system affected by frequency chirp, chromatic dispersion and polarization mode dispersion. In Proceedings of the International Workshop on Systems, Signal Processing and their Applications (WOSSPA), Tipaza, Algeria, 9–11 May 2011.
24. Baghdouche, L.K.; Simohamed, L.M. Interferometer phase error and chromatic dispersion effects on the performances of 40 Gbit/s optical DPSK transmission systems. In Proceedings of the 8th International Workshop on Systems, Signal Processing and their Applications (WoSSPA), Algiers, Algeria, 12–15 May 2013.
25. Linlin, B.; Jianming, L.; Li, L.; Xuecheng, Z. Comprehensive assessment of new modulation techniques in 40 Gb/s optical communication systems. In Proceedings of the 3rd International Photonics & Optoelectronics Meetings, Wuhan, China, 2–5 November 2010; IOP Publishing: Bristol, UK, 2011; Volume 276, pp. 1–6.
26. Malhotra, J.; Kumar, M. Performance analysis of NRZ, RZ, CRZ and CSRZ data formats in 10Gb/s optical soliton transmission link under the impact of chirp and TOD. *Opt. Int. J. Light Electron Opt.* **2010**, *121*, 800–807. [\[CrossRef\]](#)
27. Cao, H.; Atai, J.; Yu, Y.; Xiong, B.; Zhou, Y.; Cai, J.; Shu, X. Carrier-suppressed return-to-zero to non-return-to-zero format conversion based on a single fiber Bragg grating with knife-shaped spectra. *Appl. Opt.* **2014**, *53*, 5649. [\[CrossRef\]](#) [\[PubMed\]](#)
28. Cheng, K.; Conradi, J. Reduction of pulse-to-pulse interaction using alternative RZ formats in 40-Gb/s systems. *IEEE Photon. Technol. Lett.* **2002**, *14*, 98–100. [\[CrossRef\]](#)
29. Abbas, H.; Gregory, M.; Austin, M. A New Prime Code for Synchronous Optical Code Division Multiple-Access Networks. *J. Comput. Netw. Commun.* **2018**, *2018*, 3192520. [\[CrossRef\]](#)
30. Yadav, R.; Kaur, G. Design and performance analysis of 1D, 2D and 3D prime sequence code family for optical CDMA network. *J. Opt.* **2016**, *45*, 343–356. [\[CrossRef\]](#)
31. Abd, T.; Aljunid, S.; Fadhil, H.; Junita, M.; Saad, M. Impact of Multi-Diagonal Code on High-Speed Spectral Amplitude Coding Optical Code Division Multiple-Access Networks. *Arab. J. Sci. Eng.* **2013**, *38*, 2389–2397. [\[CrossRef\]](#)
32. Agrawal, G.P. *Applications of Nonlinear Fiber Optics*, 2nd ed.; Academic Press: Amsterdam, The Netherlands, 2008; pp. 319–321.
33. Agrawal, G.P. *Nonlinear Fiber Optics*, 5th ed.; Academic Press: Amsterdam, The Netherlands, 2013; pp. 397–457.
34. Ramaswami, R.; Sivarajan, K.; Sasaki, G. *Optical Networks*, 3rd ed.; Elsevier/Morgan Kaufmann: Amsterdam, The Netherlands, 2010; pp. 264–320.
35. Alsowaidi, N.; Eltaif, T.; Mokhtar, M.R. Performance analysis of a Hybrid Optical CDMA/DWDM System against Inter-Symbol Interference and Four Wave Mixing. *Digit. Commun. Netw.* **2021**, *7*, 151–156. [\[CrossRef\]](#)
36. Gnauck, A.H. Advanced Amplitude- and Phase Coded Formats for 40-Gb/s Fiber Transmission. In Proceedings of the IEEE/LEOS Annual Meeting, Rio Grande, PR, USA, 11–12 November 2004.
37. Sheetal, A.; Sharma, A.; Kaler, R.S. Impact of optical modulation formats on SPM-limited fiber transmission in 10 and 40 Gb/s optimum dispersion-managed lightwave systems. *Optik* **2010**, *121*, 246–252. [\[CrossRef\]](#)